Macromolecules

ARTICLE

pubs.acs.org/Macromolecules

Starlike Polymer Brushes

Holger Merlitz,*[,†,‡] Chen-Xu Wu,*[,†] and Jens-Uwe Sommer[‡]

[†]Department of Physics and ITPA, Xiamen University, Xiamen 361005, P.R. China

[‡]Leibniz-Institut für Polymerforschung Dresden, 01069 Dresden, Germany

ABSTRACT: We investigate the properties of polymer brushes made of symmetric and asymmetric starlike polymers in good solvent using Langevin dynamics simulations. Two types of populations coexist in such a brush, one of them being made of highly stretched polymers and a second one made of stars that are retracted inside the lower brush regions. Scaling properties of molecular tension, brush layer thickness, and brush density are in reasonable agreement with those of linear chain brushes. The dynamics of stars switching between both the retracted and the stretched states is analyzed, and an exponential scaling with the stretching energy difference is proposed. Most of our results are found in good agreement with recent SCF calculations of Polotsky et al., with one notable exception that their proposed transition from a longest path stretching mode to a uniform stretching mode, the latter being dominant at high densities, has not been supported by our data. Instead, the longest path stretching dominates at high densities as a result of a surface instability, which has previously been found with brushes made of linear chains at high grafting densities.

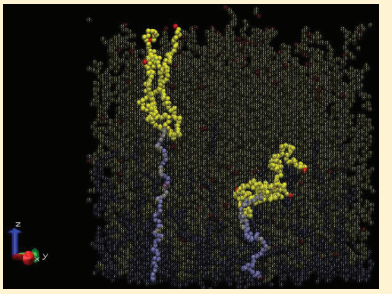

I. INTRODUCTION

Polymers that are densely grafted onto solid substrates have important applications in lubrication, adhesion, colloidal stability and biotechnology. The peculiar properties of these polymer brushes result from the interplay of chain deformation (stretching), excluded volume effects (depending on solvent quality), and additional interactions such as polymer−substrate interactions (frequently of van der Waals type) and demixing effects in polymer brushes composed of different species (mixed brushes).

Brushes made of linear chains have been intensively studied during the last three decades. Initially, there were approaches based on scaling theory, by Alexander[1] and de Gennes.[2] We refer to the review of Halperin[3] about the role of scaling approaches in polymer brushes. Alternately to scaling or mean-field-type models, self-consistent field (SCF) theory based on the strong stretching assumption was proposed by Semenov,[4] Skvortsov et al.[5] and Milner et al.[6] Subsequently these approaches have been generalized and refined to cover a broad range of systems of different properties including the finite extensibility of chains.[7−10]

On the contrary, brushes created with polymers of rather complex architectures are less well understood. Scaling properties of comb- and starlike brushes were studied by Zhulina et al.,[11] and the scaling of dendritic brushes was recently discussed by Kroeger et al.[12] Another recent work on dendritic brushes was presented by Polotsky et al.,[13] containing a concise investigation of their properties using SCF and scaling theory.

In the present work, we carry out computer simulations of starlike polymer brushes in good solvent. These brushes represent a special case of dendritic brushes; our star polymers, being made of four arms, can be regarded as dendrimers of first generation and functionality three. Both symmetric and asymmetric star architectures are employed, and the scaling properties of the resulting brush layers over a broad range of grafting densities are studied. Two populations of polymers coexist in such a brush, and their characters and conformational statistics are analyzed. Further on, the range of validity of standard scaling theory for linear brushes is studied in the context of starlike brushes. We also investigate a recently proposed model that predicts the transition from a longest path stretching mode to a uniform stretching mode when the grafting density is increased,[13] without being able to find any support for this model in our data. Finally, dynamic properties of stars flipping between stretched and retracted states are studied, and an exponential scaling of the flip rate with the stretching energy of the polymer is proposed. The rest of this work is organized as follows: In section II, the model and simulation tool is presented, followed by a description of the simulation procedure in section III. In section IV.1 we first discuss the simulation results for symmetric star brushes, and in section IV.2 the corresponding results for asymmetric stars are analyzed. A concluding discussion of our findings is offered in section V.

II. BRUSH MODEL AND SIMULATION TOOL

The polymers were created as a coarse-grained bead−spring model without explicit twist or bending potential; that is, the bonds were freely rotating and freely jointed within the limits set by excluded volume interactions with nearby monomers. The beads represent spherical monomers which interact via a shifted Lennard-Jones (LJ) potential

$$U_{\mathrm{LJ}}(r) = 4\epsilon\left[\left(\frac{d}{r}\right)^{12} - \left(\frac{d}{r}\right)^{6} - \left(\frac{d}{r_c}\right)^{12} + \left(\frac{d}{r_c}\right)^{6}\right] \quad (1)$$

Received: June 16, 2011
Revised: July 29, 2011
Published: August 12, 2011

where d stands for the bead diameter and ϵ defines the strength of the interaction. The parameter r_c is the cutoff distance. It is easily verified that without any cutoff ($r_c \rightarrow \infty$) this potential has a minimum at $r_{min} = 2^{1/6}d$ with the depth $U_{LJ}(r_{min}) = -\epsilon$. In turn, once a cutoff $r_c = 2^{1/6}d$ is implemented, the attractive contribution to this potential is eliminated and in this way monomers in good solvent are simulated, being exclusively the case for all brushes treated in this work.

The connectivity between monomers was enforced by a finite extensible nonlinear elastic (FENE) potential,[14] defined as

$$U_{FENE} = -0.5KR_0^2 \ln\left[1 - \left(\frac{r}{R_0}\right)^2\right] + 4\epsilon\left[\left(\frac{d}{r}\right)^{12} - \left(\frac{d}{r}\right)^{6}\right] + \epsilon \quad (2)$$

where the first term is attractive and extends to a maximum bond length of $R_0 = 1.5d$, whereas the second term, a Lennard-Jones potential, contributes a short-range repulsion, which is cut off at $2^{1/6}d$, the minimum of the LJ potential. The coefficient K is defined as $K = 30\ \epsilon/d^2$, well tested in earlier studies.[15] For uncharged and relaxed polymers, this parameter set leads to an average bond length of $l_{av} = 0.97d$, and we have verified that even in the case of highly tensed polymers, which emerge at high grafting densities, these average bond lengths did not exceed $0.98d$.

The substrate forms a planar wall, defining the $x-y$ plane at $z = 0$. Monomers were prohibited to penetrate the substrate through a 9−3 type LJ-wall potential

$$U_{WALL} = \epsilon\left[\frac{2}{15}\left(\frac{d}{r}\right)^{9} - \left(\frac{d}{r}\right)^{3}\right] \quad (3)$$

including a cutoff at the minimum to deliver a purely repulsive short-range potential. The polymers were grafted on this substrate, with the grafting density σ being defined as the number of grafted macromolecules per unit area.

The simulations were carried out using the open source LAMMPS molecular dynamics package.[16] In this work, the LJ system of units is used. It is defined using a model polymer with a LJ pair-potential, featuring a bead-size $d = 1$ (one length unit), a potential depth $\epsilon = 1$ (one energy unit), and a mass $m = 1$ (one mass unit). The temperature is then normalized to that energy unit (using a Boltzmann constant $k_B = 1$), and the time unit is $\tau_{LJ} = d(m/\epsilon)^{1/2}$, which is the oscillation time of a monomer inside the LJ potential, at small amplitudes so that the harmonic approximation is valid.

The equation of motion of any nongrafted monomer in the implicit solvent (neglecting any hydrodynamic interaction) is given by the Langevin equation:

$$m\frac{d^2\mathbf{r}_i}{dt^2} + \zeta\frac{d\mathbf{r}_i}{dt} = -\frac{\partial U}{\partial \mathbf{r}_i} + \mathbf{F}_i \quad (4)$$

where $m = 1$ is the monomer mass, $\mathbf{r}_i$ the position of the ith monomer, U is the total conservative potential, and $\mathbf{F}_i$ is a random external force without drift and a second moment proportional to the temperature and the friction constant ζ. In our simulations, the temperature $T = 1.2$, a time-step $\Delta t = 0.002\tau_{LJ}$, and the friction coefficient $\zeta = \tau_{LJ}^{-1}$ were implemented. The applied friction leads to an overdamped motion on length scales of the bead size, and hence to a Brownian motion under the approximation of an immobile solvent, i.e., Rouse dynamics.[17]

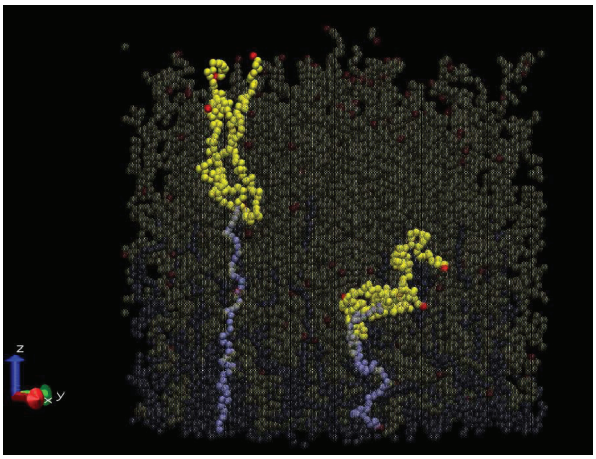

Figure 1. Snapshot: Star-polymer brush at grafting density $\sigma = 0.05$. Two exemplary molecules are highlighted, the remaining 98 molecules are made transparent to improve visibility. One of the highlighted polymers is in extended or "up" state, whereas the other one is in the retracted or "down" state.

III. SIMULATION PROCEDURE

A single arm of each star polymer (called "stem") was grafted at its end onto a substrate to form a 10×10 array of molecules. The boundaries were made periodic to eliminate finite size effects, except for the lower boundary that was defined as a solid wall with a short-range repulsion. Each system was relaxed by a simulation of 10^7 time-steps (corresponding to 2×10^5 LJ times), followed by 5×10^7 time-steps (10^6 LJ times) of data acquisition, during which a trajectory of 5000 conformations was stored for the subsequent data analysis.

In what follows, we will study brushes made of 4-arm stars at different grafting densities. First, symmetric stars (each branch having 50 monomers) are investigated. Then we consider the case of asymmetric, monodisperse stars, of which a single branch is extended through the addition of four monomers. Thus in the latter case a longest molecular path is defined. Figure 1 displays the snapshot of a typical brush conformation after relaxation (symmetric case). Two exemplary molecules are highlighted, representing an extended and a retracted conformation, respectively. Here, stem-monomers (connecting the grafting point with the branching point) are shown in blue, free branches in yellow and free ends red. Note that the vertical axis coincides with the z-coordinate, while the both x and y directions are having periodic boundary conditions.

IV. RESULTS

IV.1. Symmetric Star-Polymer Brushes. A polymer brush is primarily characterized by its density profile. For brushes made of linear chains in good solvent, the Alexander−deGennes scaling model[1,2] assumes the chain conformations to be defined by linearly aligned and densely packed correlation blobs of size of the grafting distance, i.e., $\xi \approx \sigma^{-1/2}$. On length-scales of the blob-size ξ, the chain statistics equals the statistics of chains in dilute solutions, i.e., $\xi \approx g^{\nu}$ with the Flory-exponent $\nu \approx 3/5$ in good

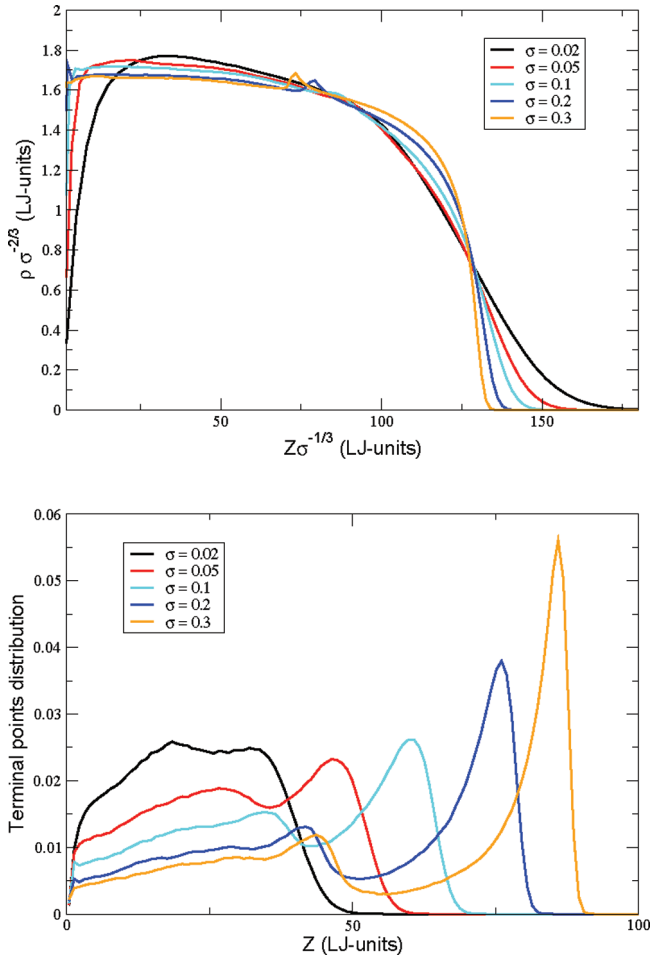

Figure 2. Symmetric star-polymer brushes: Scaled monomer-density profiles (upper panel) and terminal end distributions (lower panel) at various grafting densities.

solvent, and $g \approx \sigma^{-5/6}$ being the number of monomers per blob. This delivers the number of blobs per chain, $N/g \approx \sigma^{5/6}$ and the brush height $N\xi/g \approx \sigma^{1/3}$ as well as the monomer concentration $g\xi^{-3} \approx \sigma^{2/3}$. These scaling laws are expected to be valid for star polymers, although with different prefactors which vary with the functionality of the stars.[11,12]

In Figure 2 (upper panel) the density profiles are shown for different grafting densities σ, after scaling of the vertical coordinates with $\sigma^{-1/3}$ and the densities with $\sigma^{-2/3}$. The resulting profiles do not perfectly fall onto a master curve as they approximately do with linear polymers.[18] Yet, all profiles intersect near their inflection points, so that a plot of the layer-thickness as a function of the grafting density does in fact deliver a power-law coefficient of 1/3 just like linear chain brushes. An important anomaly is visible at high grafting densities of $\sigma \geq 0.2$: The profiles exhibit cusps near the scaled vertical coordinate of 75. Precisely these structures have been obtained before by Polotsky et al. in their SCF calculations.[13] The origin of such a cusp is the branching point of the star (or dendrimer), at which the density of the (stretched) polymer is suddenly tripled due to the transition from a single stem to three branches. At high grafting densities, the stems of the majority of stars are fully stretched out so that this branching point is strongly localized at one vertical coordinate, corresponding to the contour length of the stem. This leads to a sudden increase of the brush density that is subsequently, i.e., above the branching point, compensated by a reorganization of the branches.

Polotsky et al. have also reported a bifurcation of the dendrimer conformations into two separate populations: One population consists of strongly stretched dendrimers, whereas a subset of polymers retracts into the brush body in order to fill up the gaps that are left over in between the stems of the extended dendrimers. Such a split up into two populations should be visible as a bimodal vertical distribution of the free polymer ends, shown in Figure 2 (lower panel). A bimodal shape is clearly discernible, even at low grafting densities. Remarkable is also the tight localization of polymer ends at high grafting densities, quite similar as with brushes made of linear chains,[19] except for the coexisting, second population of retracted molecules.

In principle, the bimodal shape of star-end distributions could be a result of two different mechanisms: First, there might be fully extended polymers coexisting with retracted polymers. Second, each molecule could have a fraction of its arms reaching up to the surface and, at the same time, another fraction pointing downward to occupy the lower regions of the brush. To clarify this question, we first have to separate fully collapsed stars from the rest of the ensemble. We evaluate the average height of star ends, $\langle z_e \rangle$, and define a star to be retracted if all of its three ends occupy a region below that average $\langle z_e \rangle$. Hence, all other polymers should have at least a single arm stretched out above the average height. But this does not require every arm to point upward.

To classify the conformations, we draw an imaginary line between the branching point of a given star and the end points of each of its branches, then evaluate the angle of this line with respect to the vertical (see inset in Figure 3, upper panel). If this inclination angle is narrow, then the corresponding arm is pointing "up", if it exceeds 90°, this star end is located below the branching point and hence pointing "down".

Figure 3 displays in its upper panel normalized density distributions of these angles for the both populations. At moderate and high grafting densities, the distributions are strongly localized at low angles, indicating "hands up" conformations with all arms highly stretched above the branching point. These distributions have almost no weight at angles beyond 90°, so that the model of extended stars having both upward and downward pointing arms can be excluded. Instead, we clearly observe two populations of polymers, one of which made of molecules that are almost fully extended, the other one made of retracted polymers of far less regular shape. At low grafting densities, the differences between both populations are fuzzy. At high densities, the brush layer is so far extended that even the retracted stars are having their branches pointing up to some extent.

The separation of brush molecules into two populations is even more obvious when studying the vertical molecular tension, Figure 3 (lower panel). The "up" population consists of conformations with highly tensed stems, which, at high grafting densities, are stretched out almost to their contour lengths (i.e., 50 LJ units). SCF calculations of Polotsky et al. have come to the same conclusions.[13] Located above the highly stretched stems are the branches with considerably less tension and extension. The "down" population, however, has almost vanishing vertical forces and consequently far less regular conformations (see also Figure 1). At very high grafting density, even a slight amount of compression seems to be discernible (orange colored, dotted curve with negative vertical bond forces). Once again, at low

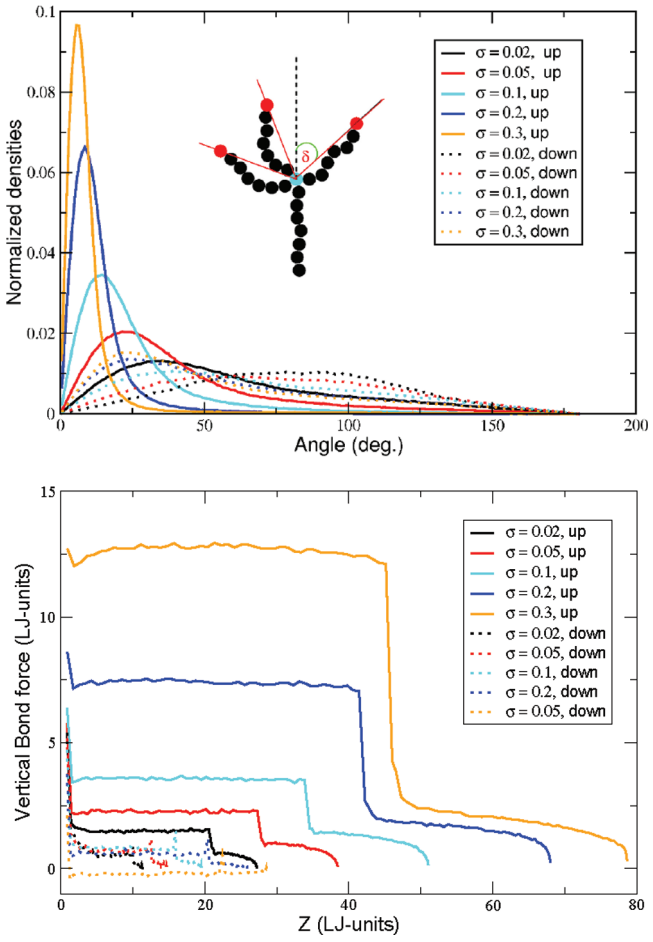

Figure 3. Two populations of stars. Upper panel: The "up" population (solid curves) has arms at narrow inclination angles above the branching point ("hands up" conformation), whereas the "down" population (dotted curves) has their arms pointing into a broad range of directions. Inset: Definition of the inclination angle. Lower panel: Vertical bond forces as a function of the average vertical monomer positions. With the "up" population, the stem is highly tensed, and rather relaxed branches. With the "down" population, the entire macromolecule is almost relaxed.

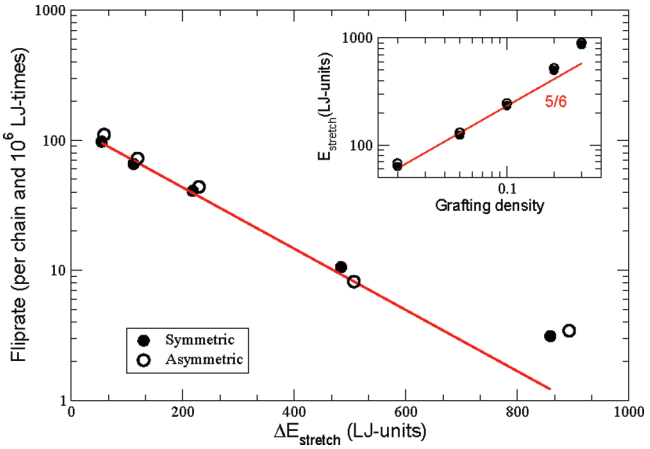

Figure 4. Flipping stars: The fliprate of stars between the two populations as a function of the stretching energy difference between up and down states. The line is an exponential fit. Inset: Stretching energy of the stars (up population) as a function of grafting density, and scaling-theory prediction for linear chains. Solid circles for symmetric stars and blank circles for asymmetric stars.

density, the two types of population are converging so that the distinction between them gradually turns fuzzy.

Considering the fact that the up-population of stars has their arms almost consistently pointing up, a somewhat stronger definition of this population appears justified: A star is "up" if all of its free ends extend above the average height (taken from the entire ensemble of both populations), and a star is "down" if all of its ends are positioned below that average. With this definition, the fraction of "up" stars increases from 30% at low grafting density ($\sigma = 0.02$) to above 50% at high density ($\sigma = 0.3$). At the same time, the fraction of "down" stars increases from 30% to 40% from low to high density. That leaves the fraction of undefined polymers shrinking from 40% at low grafting density down to 8% at high density. In other words: At high grafting densities, a polymer is either fully up or fully down, with a remaining fraction below 10% being in an undefined transition state.

The question then arises whether polymers are flipping their states between "up" and "down". A plot of the flipping rate as a function of grafting density did not deliver any power-law scaling but instead an approximate exponential decrease of that rate. This would indicate the existence of an energy barrier. The energy involved here might be the molecular stretching energy, which has the same scaling properties as the total free energy of the brush[18] and is easily obtained from the vertical bond forces (Figure 3, lower panel) through integration. For brushes made of linear chains, scaling theory predicts the free energy to scale with the number of correlation blobs, already evaluated above as being $N/g \approx \sigma^{5/6}$. The inset of Figure 4 shows that the molecular stretching energy (of the up-population) scales as $\sigma^{5/6}$ at low and moderate grafting densities, but increasingly fast at high densities. Here, the stem of the star is already stretched to its contour length and scaling theory is breaking down. As mentioned above, the down-population of stars exhibits a minor amount of stretch which hardly changes with the brush-density.

The plot of the rate of flipping as a function of the stretch-energy difference between both populations (Figure 4) reveals a negative exponential decay. This might indicate the molecular tension in fact being an important factor for the activation energy barrier. Apparently a retracted polymer has to stretch spontaneously toward the brush surface before a free energy gain is obtained due to the (abrupt) decrease in the brush potential. However, a deviation from this functional behavior exists at the highest grafting density which is not explainable with this energy alone. It appears that the flip mechanism is changing into another mode that may involve the coordinated movement of two chains in opposite directions, thereby somewhat reducing the energy barrier. In the conclusion section we are going to pick up the discussion about this interesting deviation from exponential scaling once again.

IV.2. Asymmetric Star-Polymer Brushes. We have prepared star-polymers having one of their three (free) arms extended by 4 monomers, i.e., with 54 instead of the usual 50 monomers. Such a molecule has a well-defined longest path, starting with the grafting point and extending over the stem, the branching point, and the longest branch, i.e., of length 104 (bonds). Although the overall properties of the resulting brushes remain practically the same as with the previously studied symmetric stars, there exist certain differences that are worth studying.

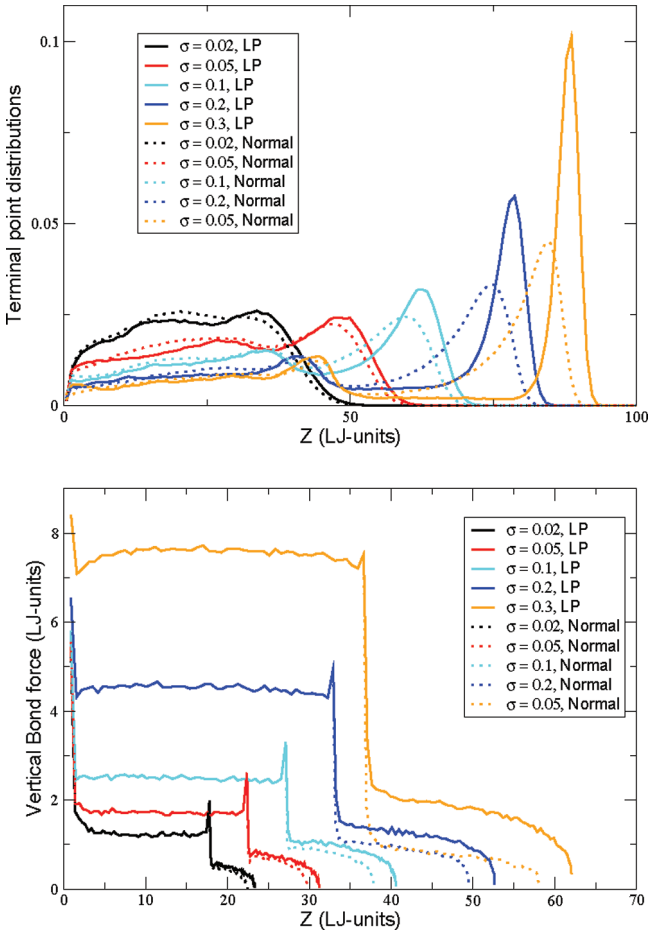

Figure 5. Asymmetric star brushes. Upper panel: With increasing grafting density σ, the end points of the longest path (LP) branches increasingly deviate from the end points of regular (normal) branches, indicating an overstretching of the extended arms. Lower panel: The vertical bond forces exhibit a significant tension of the longest path arms at high grafting densities.

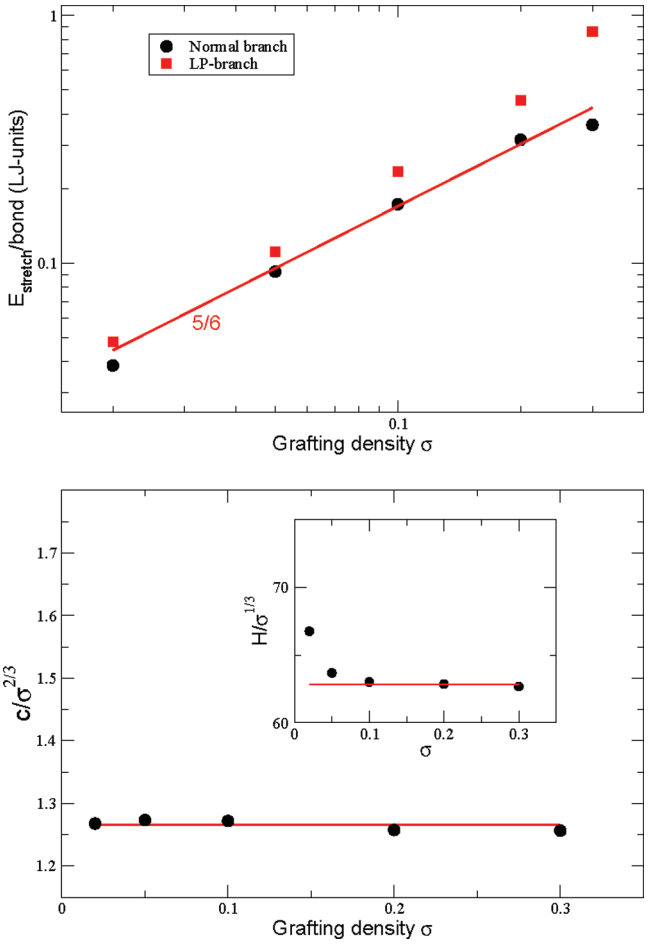

Figure 6. Asymmetric star brushes. Upper panel: Vertical stretching energy per bond, for normal branches (circles) and longest path branches (squares). The line is the scaling theory prediction for linear chains. Lower panel: Scaled brush concentration and brush center of mass height (inset) as a function of grafting density. Red lines are horizontals as predicted by scaling theory.

Figure 5 displays normalized vertical distributions of the polymer ends, after breakup into longest path and normal branches (upper panel). It is no surprise to find the longest path arms extending somewhat further than the regular arms. However, the deviations increase dramatically at high grafting density. For example, at $\sigma = 0.3$, the peak of the regular star end distribution is located at 84, and with the longest path arms it is found at 88.5, the difference being larger than the contour length of the arm extension. This implies the entire longest path arm being overstretched. Such an effect has been observed before with linear polymer brushes at high grafting densities, whenever a minority of chains was of extended length.[19] At high grafting densities, the density profiles of both linear and starlike polymer brushes are approaching a box-like shape, with diminishing density gradient inside the brush body, but high gradient near the surface at which the monomer density drops sharply. Consequently, the osmotic pressure that generates the vertical chain tension is highly localized within a narrow surface region, a phenomenon referred to as a surface instability. Such a surface instability has been shown to be supportive of the construction of switchable surfaces.[20]

A plot of the average vertical bond forces as a function of the average vertical positions displays the tension of the branches directly, Figure 5 (lower panel). Once again, the differences at high grafting densities are very significant. Note that for $\sigma = 0.3$, the tension of a normal branch (dotted orange curve) is, apart from the upper region, hardly any different from the tension at $\sigma = 0.2$ (dotted blue curve). The corresponding longest path arms, however, experience a steep increase of tension during the transition from $\sigma = 0.2$ to 0.3.

Through integration of these curves, the average vertical stretching energy per bond is obtained in Figure 6 (upper panel). Both display a power-law behavior, with a slope slightly above the prediction obtained for linear chain brushes, i.e., $E \approx \sigma^{5/6}$. At the highest grafting density, deviations occur which support the picture of a clean separation of the upper brush region into two populations: An increasingly overstretched longest path population and a second, significantly less tensioned normal population. Since the peaks of their end distributions are separated further than the difference in their contour lengths, this separation is significant and reflecting the peculiar properties of the surface instability of high density brushes.

In a recent work, Polotsky et al. have suggested a scaling model for the stretching properties of polymer brushes made of dendrimers; note that a star polymer with four arms, as studied

dx.doi.org/10.1021/ma201363u |*Macromolecules* 2011, 44, 7043–7049

in our paper, is equivalent to a first-generation dendrimer with functionality three.[13] They assumed two possible scenarios for the stretching of these polymers: First the longest path mode, in which only the longest paths are stretched, while other branches remain relaxed. Second the uniform stretching mode, in which all bonds are assumed to have identical tension. Assuming N is the number of monomers of the molecule and N_{lp} the longest path, they derive scaling-theory predictions for both scenarios, for the brush height

$$H \approx \begin{cases} N_{lp}(N/N_{lp})^{2/3}\sigma^{1/3}, & \text{longest path stretching} \\ N_{lp}(N/N_{lp})^{1/3}\sigma^{1/3}, & \text{uniform stretching} \end{cases} \quad (5)$$

and the average intrabrush concentration

$$c \approx \begin{cases} (N/N_{lp})^{1/3}\sigma^{2/3}, & \text{longest path stretching} \\ (N/N_{lp})^{2/3}\sigma^{2/3}, & \text{uniform stretching} \end{cases} \quad (6)$$

Note that for any one of the both stretching modes, scaling with the grafting density σ is identical and consistent with the scaling theory of linear brushes, but the prefactors differ, depending on the way how the polymers are stretched.

Obviously, both scenarios are simplified limit cases, and in a real system there exists a blend of both stretching modes. But Polotsky et al. assumed the longest path mode to be predominant at low grafting densities and the uniform stretching mode dominating at high densities. Corresponding SCF calculations did support such an assumption, which, however, appears to be in contradiction with our results shown in Figures 5 and Figure 6 (upper panel).

In order to investigate this case further, we have plotted scaled average brush densities, $c\sigma^{-2/3}$ and scaled brush heights $H\sigma^{-1/3}$ versus the grafting density σ. Here, we made use of $c = \sum_z c^2(z)/\sum_z c(z)$ and $H = \sum_z z\, c(z)/\sum_z c(z)$, i.e., H being the center of mass height of the brush layer. In our case, the molecule mass equals $N = 205$ and the longest path $N_{lp} = 104$, yielding $(N/N_{lp})^{1/3} \approx 1.25$ and $(N/N_{lp})^{2/3} \approx 1.57$. If a transition from longest path stretching to uniform stretching does in fact take place, then the plot of $H\sigma^{-1/3}$ vs σ should deliver a residual negative slope, and $c\sigma^{-2/3}$ vs σ should exhibit a residual positive slope. Figure 6 (lower panel) shows that no indication for such a residual slope of the scaled concentration is discernible, apparently in contradiction to the SCF results obtained by Polotsky et al. for the same system (see Figure 4b in ref 13). Our plot of the scaled brush height (inset in 6, lower panel) does in fact show an initial drop of the curve. However, this deviation from ordinary scaling theory occurs at lowermost densities. Here, there generally exists a smooth cross over from the mushroom to the brush regime, and the deviation from scaling theory at $\sigma = 0.02$ is a typical signature for such a transition. Additionally, the suggested transition from longest path scaling to uniform scaling was supposed to occur at higher densities, as observed in the SCF calculations mentioned above.

Hence, when summarizing the facts collected in Figures 5 and 6, we conclude that no support for any transition from longest path stretching to uniform stretching is found. To the contrary, the longest path arms become increasingly overstretched at high grafting densities, a consequence of the surface instability that exist with high density polymer brushes.

For the sake of completeness, the flip dynamics of asymmetric star polymer brushes has been investigated and found to be essentially identical with the results found for symmetric star brushes (Figure 4), including the deviation from exponential scaling at the highest density $\sigma = 0.3$. Hence, the different symmetries of stars used for our brushes did not significantly affect their flipping dynamics.

V. SUMMARY AND DISCUSSION

Star polymer brushes display a couple of striking differences from linear polymer brushes: Most notably the coexistence of two star populations, one of which consisting of highly stretched polymers with "hands up" conformations, the other one consisting of retracted molecules with low tension and irregular conformations (Figures 1 and 3). The emergence of two populations has been reported before in brushes made of bidisperse linear chains.[21] However, in the present case this separation occurs even when the brush is made of monodisperse polymers, being a classical example for a spontaneous symmetry breaking.

The "up" population exhibits a high bond tension of their grafted stems, while their free branches are just moderately stretched. When the molecules are asymmetric, then their longest paths are consistently overstretched, particularly in the high density regime (Figure 5). This is consistent with previous studies of linear brushes and the consequence of a surface instability that occurs with densely grafted brushes,[19] but in apparent contradiction with recently published SCF results, which suggested a gradual transformation from longest path to uniform stretching.[13] It is, at this stage, impossible to speculate about reasons for the observed differences. Obviously one might first of all take a look at the implementation of the bond forces; the SCF model applies freely jointed polymers on a lattice, and their effective elastic properties under high tension are likely to differ from the FENE type bond force in our continuous model. The observed differences are interesting and shall trigger further research. In most other aspects, like the existence of two polymer populations, overstretched stems, even details such as certain anomalies of the monomer density distributions (Figure 2), both the SCF results and our simulations display close similarities.

It is worth mentioning that many of the scaling predictions for linear chain brushes still remain valid for star polymer brushes (Figures 2, 4, and 6). This has been predicted to be the case,[11,12] but to the best knowledge of the authors, never been verified in detail through molecular simulations. Our data did also reveal the limitations of the scaling approach: Deviations from scaling theory consistently occurred at high densities, when the molecule stems were overstretched so that the blob picture was breaking down.

Polymers are able to flip between stretched and retracted states, and these flips are exponentially suppressed with increasing grafting density. This suggests an activation energy barrier, and such a barrier would certainly scale with the stretching energy difference of the both states. This seems to be the case (Figure 4), however, there exists a significant deviation from that exponential suppression of the fliprate at very high grafting density. Even more surprising is the fact that those flips occur more often, not less often, than expected, whereas notorious suspects like friction or entanglement, both of which would turn more effective at high densities, should yield the opposite result. Perhaps, at these long time scales, another flip mechanism becomes efficient that requires a lower energy barrier, e.g., through the simultaneous motion of two chains in opposite directions. Or, at such a high density, stars belonging to the retracted population are already stretched out and therefore rather streamline. The distribution of inclination angles in Figure 3 would

support such an explanation; however, in this case a significant deviation from exponential scaling should be visible already at $\sigma = 0.2$ at which the stars are quite a bit stretched up either. Further detailed investigations of the flip mechanism at high densities are required, and they will ask for a significant computational investment since these switch events, and hence molecules in a transition state, are rare.

AUTHOR INFORMATION

Corresponding Author

*E-mail: merlitz@gmx.de; cxwu@xmu.edu.cn.

ACKNOWLEDGMENT

This work was partly supported by the National Science Foundation of China under Grant No. 10225420 and 11074208 and by the DFG priority program SPP 1369.

REFERENCES

(1) Alexander, S. *J. Phys. (France)* **1977**, *38*, 977.
(2) deGennes, P. *Macromolecules* **1980**, *13*, 1069.
(3) Halperin, A. In *Soft Order in Physical Systems*; NATO ASI Series; Bruinsma, R., Rabin, Y., Eds.; Plenum Press: New York, 1994; p 33.
(4) Semenov, A. *JETP Lett.* **1985**, *85*, 733.
(5) Skvortsov, A. M.; Pavlushkov, I. V.; Gorbunov, A. A.; Zhulina, E. B.; Borisov, O. V.; Pryamitsyn, V. A. *Polym. Sci. U.S.S.R.* **1988**, *30*, 1706.
(6) Milner, S.; Witten, T.; Cates, M. *Macromolecules* **1988**, *21*, 1610.
(7) Shim, D.; Cates, M. *J. Phys. (Paris)* **1989**, *50*, 3535.
(8) Amoskov, V. M.; Pryamitsyn, V. A. *J. Chem. Soc. Faraday Trans.* **1994**, *90*, 889.
(9) Lai, P.-Y.; Halperin, A. *Macromolecules* **1991**, *24*, 4981.
(10) Biesheuvel, P. M.; deVos, W. M.; Amoskov, V. M. *Macromolecules* **2008**, *42*, 6254.
(11) Zhulina, E.; Vilgis, T. *Macromolecules* **1995**, *28*, 1008.
(12) Kroeger, M.; Peleg, O.; Halperin, A. *Macromolecules* **2010**, *43*, 6213.
(13) Polotsky, A. A.; Gillich, T.; Borisov, O. V.; Leermakers, F. A. M.; Textor, M.; Birshtein, T. M. *Macromolecules* **2010**, *43*, 9555.
(14) Kremer, K.; Grest, G. *J. Chem. Phys.* **1990**, *92*, 5057.
(15) Murat, M.; Grest, G. *Phys. Rev. Lett.* **1989**, *63*, 1074.
(16) Plimpton, S. *J. Comput. Phys.* **1995**, *117*, 1. http://lammps.sandia.gov/.
(17) Rouse, P. *J. Chem. Phys.* **1953**, *21*, 1272.
(18) He, G.-L.; Merlitz, H; Sommer, J.-U.; Wu, C.-X. *Macromolecules* **2007**, *40*, 6721.
(19) Merlitz, H.; He, G.-L.; Wu, C.-X.; Sommer, J.-U. *Macromolecules* **2008**, *41*, 5070.
(20) Merlitz, H.; He, G.-L.; Wu, C.-X.; Sommer, J.-U. *Phys. Rev. Lett.* **2009**, *102*, 115702.
(21) Skvortsov, A. M.; Klushin, L. I.; Gorbunov, A. A. *Macromolecules* **1997**, *30*, 1818.